

# AGFSync: Leveraging AI-Generated Feedback for Preference Optimization in Text-to-Image Generation

Jingkun An<sup>1,3,\*</sup>, Yinghao Zhu<sup>1,\*</sup>, Zongjian Li<sup>2,3,\*</sup>, Haoran Feng<sup>1</sup>,  
Bohua Chen<sup>3</sup>, Yemin Shi<sup>4</sup>, and Chengwei Pan<sup>1,†</sup>

<sup>1</sup> Beihang University, Beijing, China

<sup>2</sup> Huazhong University of Science and Technology, Wuhan, China

<sup>3</sup> Shenzhen RabbitPre Intelligent Technology, Guangdong, China

<sup>4</sup> Peking University, Beijing, China

\* Equal contribution    † Corresponding author  
shiyemin@pku.edu.cn    pancw@buaa.edu.cn

**Abstract.** Text-to-Image (T2I) diffusion models have achieved remarkable success in image generation. Despite their progress, challenges remain in both prompt-following ability, image quality and lack of high-quality datasets, which are essential for refining these models. As acquiring labeled data is costly, we introduce **AGFSync**, a framework that enhances T2I diffusion models through Direct Preference Optimization (DPO) in a fully AI-driven approach. **AGFSync** utilizes Vision-Language Models (VLM) to assess image quality across style, coherence, and aesthetics, generating feedback data within an AI-driven loop. By applying **AGFSync** to leading T2I models such as SD v1.4, v1.5, and SDXL, our extensive experiments on the TIFA dataset demonstrate notable improvements in VQA scores, aesthetic evaluations, and performance on the HPSv2 benchmark, consistently outperforming the base models. **AGFSync**'s method of refining T2I diffusion models paves the way for scalable alignment techniques.

**Keywords:** Text-to-Image Generation, Diffusion Models, Direct Preference Optimization, AI Feedback

## 1 Introduction

The advent of Text-to-Image (T2I) generation technology represents a significant advancement in generative AI. Recent breakthroughs have predominantly utilized diffusion models to generate images from textual prompts [2, 17, 23, 31]. However, achieving high fidelity and aesthetics in generated images continues to pose challenges, including deviations from prompts and inadequate image quality [30]. Addressing these challenges requires enhancing diffusion models' ability to accurately interpret detailed prompts (prompt-following ability [2]) and improve the generative quality across style, coherence, and aesthetics.

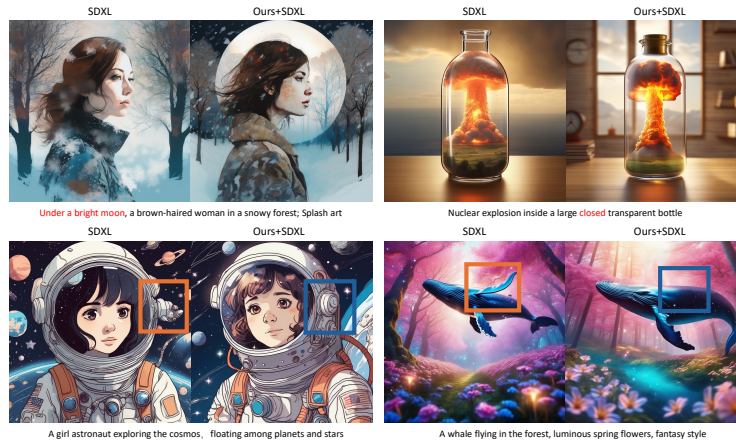


**Fig. 1:** We introduce **AGFSync**: a model-agnostic training algorithm that improves text-to-image (T2I) generation models’ faithfulness and coherence to text inputs and image aesthetics without human interventions. The images showcase a comparison of the results before and after fine-tuning SDXL with **AGFSync**.

Efforts to overcome these challenges span dataset, model, and training levels. High-quality text-image pair datasets, as proposed in the data-centric AI philosophy, can significantly improve performance [32]. Therefore a high-quality image caption, and its corresponding image pair dataset is crucial in training [2]. At the model architecture level, advancements include the optimization of cross-attention mechanisms to improve model compliance [7]. These efforts, both at the dataset and model architecture levels, follow the traditional training paradigm of using elaborately designed models with specific datasets. In contrast, in the training domain, strategies inspired by the success of large language models, such as OpenAI’s ChatGPT [14], include supervised fine-tuning (SFT) and alignment stages. With a pretrained T2I diffusion model, enhancing the model for better image quality can be approached in either the SFT stage or the alignment stage. The former approach, as seen in the latest work DreamSync [26], fine-tunes the diffusion model through a selected image selection procedure where a Vision-Language Model (VLM) evaluates and then selects high-quality text-image pairings for further fine-tuning. However, DreamSync exhibits a lower prompt generation conversion rate and is limited by the intrinsic capabilities of the diffusion model, leading to uncontrollable data distribution in the fine-tuning dataset. The latter approach, DPOK [6], DDPO [3], and DPO [20] use reinforcement learning for alignment, while Diffusion-DPO [27] applies Direct Preference Optimization (DPO) for model alignment, modifying the original DPO algorithm to directly optimize diffusion models based on preference data. Yet, it only focuses on evaluating image quality from one aspect. Furthermore, existing methods mostly depend on extensive, quality-controlled labeled data.

Addressing these requires a cost-effective, low-labor approach that minimizes the need for human-labeled data while considering multiple quality aspects of images. Leveraging AI in generating datasets and evaluating image quality can fulfill these gaps without human intervention. Through generating diverse textual prompts, assessing generated images, and constructing a comprehensive preference dataset, **AGFSync** epitomizes the full spectrum of AI-driven innovation—ushering in an era of enhanced data utility, accessibility, scalability, and process automation while simultaneously mitigating the costs and limitations associated with manual data labeling.

More specifically, **AGFSync** aligns text-to-image diffusion models via DPO, with multi-aspect AI feedback generated data. The process begins with the preference candidate set generation, where LLM generates descriptions of diverse styles and categories, serving as high-quality textual prompts. Candidate images are then generated using these AI-generated prompt, therefore constructing candidate prompt-image pairs. Image evaluation and VQA data construction follow, using LLM to generate questions related to the composition elements, style, etc., based on its initial prompts. VQA scoring is conducted by inputting these questions into the VQA model to assess whether the diffusion model-generated images aesthetically follow the prompts, calculating accuracy as the VQA score. With combined weighted scores of VQA, CLIP, and aesthetics filtering, the preference pair dataset is established within the best and worst images. Finally, DPO alignment is applied to the diffusion model using the constructed preference pair dataset. The entire process leverages the robust capabilities of VLMs without any human engagement, ensuring a human-free, cost-effective workflow.

Our contributions are summarized as follows:

1. We introduce an openly accessible dataset composed of 45.8K AI-generated prompt samples and corresponding SDXL-generated images, each accompanied by question-answer pairs that validate the image generation’s fidelity to textual prompts. This dataset not only propels forward the research in T2I generation but also embodies the shift towards higher data utilization, scalability, and generalization, signifying a breakthrough in mitigating the unsustainable practices of manual data annotation.
2. Our proposed framework **AGFSync**, aided by multiple evaluation scores, leveraging DPO fine-tuning approach, introduces a fully automated, AI-driven approach, which elevates fidelity and aesthetic quality across varied scenarios without human annotations.
3. Extensive experiments demonstrate that **AGFSync** significantly and consistently improves upon existing diffusion models in terms of adherence to text prompts and overall image quality, establishing the efficacy and transformative potential of our AI-driven data generation, evaluation and fine-tuning framework.

## 2 Related Work

### 2.1 Aligning Diffusion Models Methods

The primary focus of related work in this area is to enhance the fidelity of images generated by diffusion models in response to text prompts, ensuring they align more closely with human preferences. This endeavor spans across dataset curation, model architecture enhancements, and specialized training methodologies.

**Dataset-Level Approaches:** A pivotal aspect of improving image generation models involves curating and fine-tuning datasets that are deemed visually appealing. Works by [17, 22] utilize datasets rated highly by aesthetics classifiers [24] to bias models towards generating visually appealing images. Similarly, Emu [5] enhances both visual appeal and text alignment through fine-tuning on a curated dataset of high-quality photographs with detailed captions. Efforts to re-caption web-scraped image datasets for better text fidelity are evident in [2, 25]. Moreover, DreamSync [26] improves T2I synthesis with feedback from vision-language image understanding models, aligning images with textual input and the aesthetic quality of the generated images.

**Model-Level Enhancements:** At the model level, enhancing the architecture with additional components like attention modules [7] offers a training-free solution to enhance model compliance with desired outputs. StructureDiffusion [7] and SynGen [21] also work on training-free methods that focus on model’s inference time adjustments.

**Training-Level Strategies:** The integration of supervised fine-tuning (SFT) with advanced alignment stages, such as reinforcement learning approaches like DPOK [6], DDPO [3], and DPO [20], demonstrates significant potential in aligning image quality with human preferences. Among these, Diffusion-DPO emerges as an RL-free method, distinct from other RL-based alignment strategies, effectively enhancing human appeal while ensuring distributional integrity [27].

Common drawbacks of them is the expensive fine-tuning dataset where most of these approaches rely on human-annotated dataset and human evaluation. This paradigm cannot support training an extensive and scalable diffusion model.

### 2.2 Image Quality Evaluation Methods

Evaluating image quality in a comprehensive manner is pivotal, integrating both automated benchmarks and human assessments to ensure fidelity and aesthetic appeal. The introduction of TIFA [9] utilize Visual Question Answering (VQA) models to measure the faithfulness of generated images to text prompts, setting a foundation for subsequent innovations. The CLIP score [8] builds upon CLIP [19] enables a reference-free evaluation of image-caption compatibility through the computation of cosine similarity between image and text embeddings, showcasing high correlation with human judgments without needing reference captions. PickScore [11] leverages user preferences to predict the appeal of generated images, combining CLIP model elements with InstructGPT’s reward model objectives [15] for a nuanced understanding of user satisfaction. Alongside, the aes-



thetic score [10] assesses images based on aesthetics learned from image-comment pairs, providing a richer evaluation that includes composition, color, and style.

### 3 Methodology

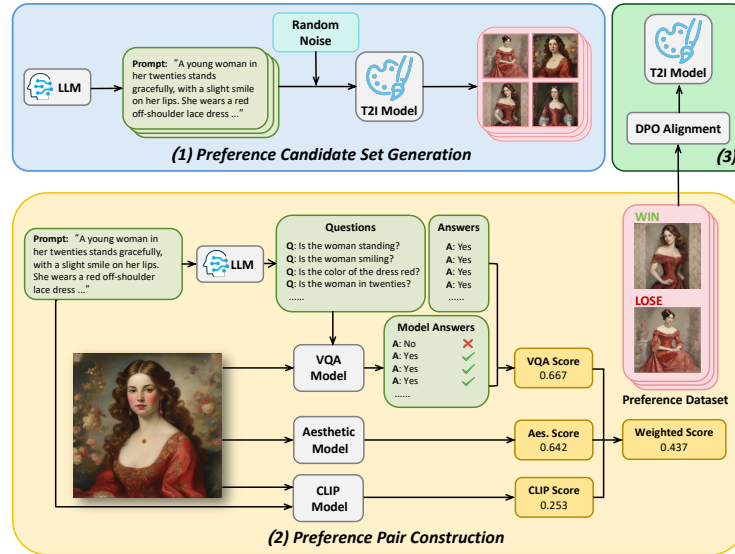


**Fig. 2:** Overall pipeline of AGFSync, which mainly encompasses 3 steps: (1) Preference Candidate Set Generation, (2) Preference Pair Construction, (3) DPO Alignment. Overall, AGFSync learns from AI generated feedback data with DPO. AGFSync requires no human annotation, model architecture changes, or reinforcement learning.

The overall pipeline of our proposed AGFSync is illustrated as in Fig. 2.

#### 3.1 Preference Candidate Set Generation

To encourage the diffusion model generate diverse style images for further text-image pair preference dataset, we intuitively think about using LLM to construct prompts that serve as image captions  $\mathbf{c}$ .

We employ LLM to generate prompts  $\mathbf{c}$  from the instruction that would further feed into T2I diffusion model. We encourage the LLM to generate 12 distinct categories for diversity: Natural Landscapes, Cities and Architecture, People, Animals, Plants, Food and Beverages, Sports and Fitness, Art and Culture, Technology and Industry, Everyday Objects, Transportation, and Abstract and Conceptual Art. The established 45.8K dataset’s statistics is in Tab. 3.

For each category, we utilize in-context learning strategy – carefully craft 5 high-quality examples aimed at guiding the large language model to grasp

the core characteristics and contexts of each category, thereby generating new prompts with relevant themes and rich content. Additionally, we emphasize the diversity in prompt lengths, aiming to produce both succinct and elaborate prompts to cater to different generational needs and usage scenarios.

To construct the preference candidate set, we consider a text-conditioned generative diffusion model  $G$  for candidate the image generation, where  $G$  accept input parameters: text condition  $\mathbf{c}$  and latent space noise  $\mathbf{z}_0$ . We let the diffusion model to generate  $N_{\mathbf{c}}$  candidate images. To enhance the diversity and distinctiveness of the images produced by the model, we incorporate unit Gaussian noise into the conditional input  $\mathbf{c}$  and generate  $\mathbf{z}_0$  with different random seeds. This approach aims to introduce more randomness and variation to avoid overly uniform or similar generated images. Specifically, the process of generating backup images can be represented as in Eq. (1):

$$\mathbf{x}_0 = G(\mathbf{c} + \mathbf{n}, \mathbf{z}_0) \quad (1)$$

where Gaussian noise  $\mathbf{n} \sim \mathcal{N}(0, \sigma^2 \mathbf{I})$  is added to the conditional input, increasing the diversity of images.

In practice, by adjusting the value of variance  $\sigma$  and using different random seeds to generate  $\mathbf{z}_0$ , the diversity of the generated images can be controlled. A larger  $\sigma$  value will lead to greater variability in the conditionality of the input, but potentially producing more diverse images but might also decrease the relevance of the image to the condition.

Therefore, currently we have preference candidate  $\mathbf{c}$  and its corresponding  $N_{\mathbf{c}}$  generated images. We will select and refine these candidates for constructing the final preference pair dataset.

### 3.2 Preference Pair Construction

**VQA Questions Generation** We also employ the LLM to refine the prompts generated for T2I generation into a series of question-and-answer pairs (QA pairs). By letting Visual Question Answering (VQA) model to answer these questions based on the generated images, the VQA score is calculated. We will establish the preference pair according to multiple image quality scores later.

To make the score easier to calculate, we ensure that the answers to these questions are uniformly "yes" in the instruction prompt. To refine the questions, we let the LLM to validate the questions if they are ambiguous or unrelated to the captions, therefore all questions are generated not valid or closely related to the text for answering by the validation process in the instruction prompt.

**VQA Score** The VQA score is computed by evaluating the correctness of answers provided by the VQA model to the questions generated from the text prompt  $\mathbf{c}$ . For each text prompt  $\mathbf{c}$ , the set of QA pairs is denoted as  $\{(Q_i(\mathbf{c}), A_i(\mathbf{c}))\}$  for  $i = 1, \dots, N_{\mathbf{c}}$ , where  $N_{\mathbf{c}}$  is the total number of QA pairs generated for the text prompt  $\mathbf{c}$ , and  $\mathbf{x}_0$  represents the image generated from  $\mathbf{c}$ .

The VQA model  $\Phi$  is employed to answer all questions  $Q_i(\mathbf{c})_{i=1}^{N_c}$  based on the image  $\mathbf{x}_0$ . The correctness of the VQA model’s answers is evaluated by comparing them to the correct answers  $A_i(\mathbf{c})$ . The VQA score [9], which quantifies the consistency between the text and the generated image, is calculated in Eq. (2):

$$s_{\text{VQA}} = \frac{1}{N_c} \sum_{i=1}^{N_c} \begin{cases} 1 & \text{if } \Phi(\mathbf{x}_0, Q_i(\mathbf{c})) = A_i(\mathbf{c}), \\ 0 & \text{otherwise.} \end{cases} \quad (2)$$

Here, the case structure explicitly represents the indicator function, which is 1 if the VQA model’s answer matches the correct answer  $A_i(\mathbf{c})$ , and 0 otherwise.

**CLIP Score** Utilizing the CLIP [19] model, we convert the prompt words and the generated image into vector representations, denoted as  $\mathbf{c}^{(emb)}$  for text and  $\mathbf{x}'_0$  for the image. The cosine similarity between the two vectors, computed in a shared embedding space, quantifies the alignment between the text and the image, embodying the CLIP Score [8]. The formula is refined as Eq. (3).

$$s_{\text{CLIP}} = \cos(\mathbf{c}^{(emb)}, \mathbf{x}'_0) = \left( \frac{\mathbf{c}^{(emb)}}{\|\mathbf{c}^{(emb)}\|_2} \cdot \frac{\mathbf{x}'_0}{\|\mathbf{x}'_0\|_2} \right) * \gamma \quad (3)$$

**Aesthetic Score** The aesthetic score assesses an image’s visual appeal by analyzing multifaceted elements like composition, color harmony, style, and high-level semantics, which collectively contribute to the aesthetic quality of an image [10]. The evaluation is represented in Eq. (4):

$$s_{\text{Aesthetic}} = \text{AestheticModel}(\mathbf{x}_0) \quad (4)$$

where  $\mathbf{x}_0$  signifies the input image, and  $\text{AestheticModel}(\cdot)$  refers to a sophisticated model function that yields a score reflecting the image’s aesthetic appeal on a normalized scale. Higher scores denote a greater aesthetic appeal.

**Weighted Score Calculation** Consider a set of scores  $\{s_1, s_2, \dots, s_n\}$ , where each score  $s_i$  corresponds to a distinct evaluation metric utilized. Alongside these scores, let there be a set of weights  $W = \{w_1, w_2, \dots, w_n\}$ , with each weight  $w_i$  specifically assigned to modulate the influence of its corresponding score  $s_i$ .

The composite score for an image  $\mathbf{x}_0$ , which integrates these diverse evaluation metrics, is determined by calculating the sum of the weighted scores. The formula for computing this aggregated score is given by Eq. (5):

$$S(\mathbf{x}_0) = \sum_{i=1}^n w_i s_i(\mathbf{x}_0) \quad (5)$$

where  $n$  represents the total number of individual scores. The weighted sum approach facilitates the model’s capability to assess images across varied criteria, offering a comprehensive understanding of the image’s quality and relevance.

**Preference Pair Dataset Construction** With the previous generated set of  $N$  images  $\mathbf{X}_0 = \{\mathbf{x}_0^1, \mathbf{x}_0^2, \dots, \mathbf{x}_0^N\}$  for a given textual prompt  $\mathbf{c}$ , each candidate image is then evaluated to assign the score calculated in multiple aspects as the aforementioned weighted score. To identify the most and least preferred images, which we term as the "winner" and "loser", we employ the following selection criteria in Eq. (6) and Eq. (7):

$$\mathbf{x}_0^w = \arg \max_{\mathbf{x}_0^i \in \mathbf{X}_0} S(\mathbf{x}_0^i) \quad (6)$$

$$\mathbf{x}_0^l = \arg \min_{\mathbf{x}_0^i \in \mathbf{X}_0} S(\mathbf{x}_0^i) \quad (7)$$

This approach yields a preference pair for each textual prompt  $\mathbf{c}$ , represented as  $(\mathbf{c}, \mathbf{x}_0^w, \mathbf{x}_0^l)$ . The rationale behind selecting the highest and lowest scored images is to capture the widest possible discrepancy in quality and relevance, providing a clear contrast suitable for fine-tuning with DPO.

### 3.3 DPO Alignment

Derive from Diffusion-DPO [20], we consider the preference dataset, denoted as  $\mathcal{D} = \{(\mathbf{c}, \mathbf{x}_0^w, \mathbf{x}_0^l)\}$ . Applying DPO for diffusion models is modeled as the following objective function Eq. (8). For the detailed notation of algorithms Eq. (8), please refer to Diffusion-DPO [20] and DPO [20].

$$\begin{aligned} L_{\text{Diffusion-DPO}}(\theta) = & -\mathbb{E}_{(\mathbf{x}_0^w, \mathbf{x}_0^l) \sim \mathcal{D}, t \sim \mathcal{U}(0, T), \mathbf{x}_t^w \sim q(\mathbf{x}_t^w | \mathbf{x}_0^w), \mathbf{x}_t^l \sim q(\mathbf{x}_t^l | \mathbf{x}_0^l)} \\ & \log \sigma(-\beta T \omega(\lambda_k) (\|\boldsymbol{\epsilon}^w - \boldsymbol{\epsilon}_\theta(\mathbf{x}_t^w, t, \mathbf{c})\|_2^2 - \|\boldsymbol{\epsilon}^w - \boldsymbol{\epsilon}_{\text{ref}}(\mathbf{x}_t^w, t, \mathbf{c})\|_2^2 \\ & - (\|\boldsymbol{\epsilon}^l - \boldsymbol{\epsilon}_\theta(\mathbf{x}_t^l, t, \mathbf{c})\|_2^2 - \|\boldsymbol{\epsilon}^l - \boldsymbol{\epsilon}_{\text{ref}}(\mathbf{x}_t^l, t, \mathbf{c})\|_2^2))) \end{aligned} \quad (8)$$

where  $\mathbf{x}_t^* = \alpha_t \mathbf{x}_0^* + \sigma_t \boldsymbol{\epsilon}^*$ ,  $\boldsymbol{\epsilon}^* \sim \mathcal{N}(0, \mathbf{I})$ . Here,  $\alpha_t$  and  $\sigma_t$  are the noise scheduling functions as defined in [23]. Consequently,  $\mathbf{x}_t \sim q(\mathbf{x}_t | \mathbf{x}_0) = \mathcal{N}(\mathbf{x}_t; \alpha_t \mathbf{x}_0, \sigma_t^2 \mathbf{I})$ . Similar to [27], we incorporate  $T$  and  $\omega(\lambda_k)$  into the constant  $\beta$ .

## 4 Experimental Setups

### 4.1 Datasets

To evaluate whether our AGFSync can enhance the performance of text-to-image models across a wide range of prompts, we considered the following benchmarks:

1. **TIFA [9]:** Based on the correct answers to a series of predefined questions. TIFA employs visual question answering (VQA) models to determine if the content of generated images accurately reflects the details of the input text. The benchmark itself is comprehensive, encompassing 4,000 different text prompts and 25,000 questions across 12 distinct categories.

2. **HPS v2 [28]**: Human Preference Score v2 (HPS v2) is an extensive dataset specifically collected to document human preference choices across a variety of images. HPD v2 aims at precisely capturing human preferences for images generated from textual descriptions. HPS v2 provides a benchmark for text-to-image generation models, with a publicly available test dataset comprising 3,200 distinct image captions, covering five types of image descriptions: anime, photo, drawbench, concept-art, and paintings.

## 4.2 Hyperparameters

For each given text prompt  $\mathbf{c}$ , we let the diffusion model generate  $N = 8$  samples as backup images for further preference dataset constitution. The weight term in the calculation of CLIP score  $\gamma$  is set to 100, which leads the CLIP Score range between 0 and 100. We also rescale the VQA score and aesthetic score to 0 – 100 by multiplying 100 to original score.

The weighting of each score measurements is allocated as:  $w_{\text{VQA}} = 0.35$ ,  $w_{\text{CLIP}} = 0.55$ ,  $w_{\text{Aesthetic}} = 0.1$ . Thus, the weighted score  $S$  for an image  $\mathbf{x}$  is calculated as Eq. (9):

$$S(\mathbf{x}) = w_{\text{VQA}}s_{\text{VQA}}(\mathbf{x}) + w_{\text{CLIP}}s_{\text{CLIP}}(\mathbf{x}) + w_{\text{Aesthetic}}s_{\text{Aesthetic}}(\mathbf{x}) \quad (9)$$

During DPO alignment stage, we finetune the original diffusion model. For SD v1.4 and SD v1.5 model, the learning rate is 5e-7, the batch size is 128, the output image size is 512\*512. For SDXL model, the learning rate is 1e-6, the batch size is 64, the output image size is 1024\*1024. We fine-tune the diffusion model for 1000 steps. The random seed is 200 in Fig. 6, Fig. 5, and Fig. 1.

## 4.3 Baseline Models and Utilized Models

We evaluated our framework, AGFSync, using Stable Diffusion v1.4 (SD v1.4), Stable Diffusion v1.5 (SD v1.5) [22], and SDXL (SDXL-base-1.0) [17], widely acknowledged in related research as the current leading open-source text-to-image (T2I) models. For prompt construction, we employ ChatGPT (GPT-3.5) [14]. For generating question-answer pairs, we use Gemini Pro [16]. Both are accessed through their official API. In addition, we adopt *Salesforce/blip2-flan-t5-xxl* for VQA scoring model [12], *openai/clip-vit-base-patch16* for evaluating CLIP score [8], *Vila* [10] for calculating aesthetic score [10], which are consistent with the baseline methods’ settings. We also employ GPT-4 Vision (GPT-4V) [1] to simulate human preference when evaluating the image quality.

## 5 Experimental Results

We present the evaluation results of baseline models fine-tuned with our framework AGFSync on benchmarks.

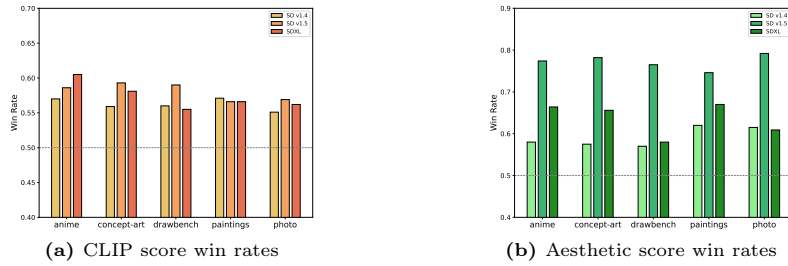


**Fig. 3:** Comparison of the win rates of SD v1.4, SD v1.5 and SDXL with or without our AGFSync on HPS v2. CLIP score (left) and aesthetic score (right).

### 5.1 Benchmarking Results on HSP v2

**Evaluate by CLIP Score and Aesthetic Score** As in Fig. 3, we test the win rates of models fine-tuned with our method AGFSync and the original models on CLIP score and aesthetic score in the HSP v2 benchmark. The experimental results demonstrate with AGFSync, models have a consistent higher win rate against the original the baseline SD v1.4, SD v1.5, and SDXL models without fine-tuning across a wide range of image descriptions. Notably, following AGFSync fine-tuning, the SDXL model achieves a win rate of 60.5% in CLIP score compared to the original model in the anime category images, and the SD v1.5 model achieves a win rate of 77.4% in aesthetic score for the photo category images. The average win rate of CLIP Score and aesthetic score for the three models increased to 57.2% and 61.6% compared to base ones.

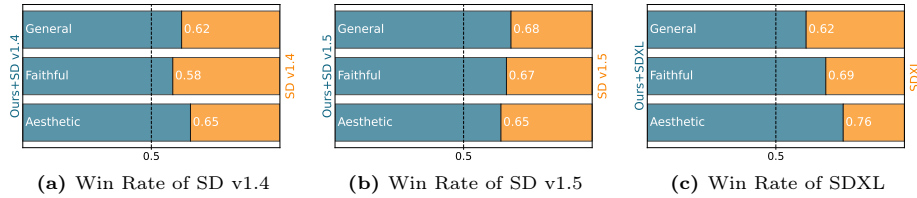


**Fig. 4:** Win rate results of using GPT-4V to evaluate our AGFSync fine-tuned models of SD v1.4, SD v1.5, and SDXL, compared to the original models for general preference (Q1), prompt alignment (Q2), and visual appeal (Q3) on the HSP v2 dataset.

**Evaluate by GPT-4 Vision to Simulate Human Preference** In this study, we explore the efficacy of AGFSync in enhancing image generation models, leveraging the capabilities of GPT-4 Vision (GPT-4V) as reported by OpenAI in 2023 [1] to simulate human preference. Our methodology involves a comparative analysis between images produced by diffusion models before and after the

application of AGFSync. These images, accompanied by their respective descriptions, were submitted to GPT-4V for evaluation based on three critical aspects: **General Preference (Q1)**: "Which image do you prefer?"; **Prompt Alignment (Q2)**: "Which image better fits the text description?"; **Visual Appeal (Q3)**: "Disregarding the prompt, which image is more visually appealing?". The evaluation process involved collecting and analyzing the frequency with which images produced by both the original and the trained model are favored under each question category. The results of this comparative analysis are visually represented in Fig. 4, which sequentially displays the performance metrics. The performance reveals that adding AGFSync yields substantial enhancements across all models concerning Q1, Q2 and Q3. Notably, with our AGFSync applied, we achieve an average of 62%, 67%, and 69% win rate of three aspects for the SD v1.4, SD v1.5, and SDXL models respectively. These results demonstrate the effectiveness of AGFSync in enhancing performance under various prompts.

## 5.2 Benchmarking Results on TIFA

**Table 1:** Results of different alignment methods on VQA score and aesthetic score on the TIFA benchmark. **Red** indicates improvement, while **Green** indicates a decrease. The best scores for each model type are highlighted in **Bold**. Column "Sum" denotes the sum of improvements on  $s_{VQA}$  and  $s_{Aes}$ .

Model	Alignment	$s_{VQA}$	$s_{Aes}$	Sum	
SD v1.4	No alignment	76.6	44.6	-	
	Training-Free	SynGen	76.8 (+0.2)	42.4 (-2.2)	-2.0
		StructureDiffusion	76.5 (-0.1)	41.5 (-3.1)	-3.0
	RL	DPOK	76.4 (-0.2)	<b>46.5 (+1.9)</b>	+1.7
		DDPO	76.7 (+0.1)	43.5 (-1.1)	-1.0
	Self-Training	DreamSync	77.6 (+1.0)	44.9 (+0.3)	+1.3
		<b>AGFSync (Ours)</b>	<b>77.9 (+1.3)</b>	47.9 (+3.3)	<b>+4.6</b>
SD v1.5	No alignment	77.1	48.0	-	
	<b>AGFSync (Ours)</b>	<b>78.7 (+1.6)</b>	<b>49.1 (+1.1)</b>	<b>+2.7</b>	
SDXL	No alignment	82.0	60.9	-	
	<b>AGFSync (Ours)</b>	<b>83.3 (+1.3)</b>	<b>65.2 (+4.3)</b>	<b>+5.5</b>	

Note: Due to the code of DreamSync not being open-sourced, the results of SD v1.4 are extracted from the DreamSync paper. We reproduce the results of SD v1.5 and SDXL. We do not apply the Refiner for SDXL. We ensure that the comparisons are fair.



In Tab. 1, We further test our method on TIFA benchmark, highlighting AGFSync’s SOTA performance on VQA score and aesthetic score over other latest SOTA alignment methods. Specifically, we compare three types of alignment methods: training-free approaches capable of modifying outputs without retraining the model, such as StructureDiffusion [7] and SynGen [21]; reinforcement learning (RL)-based methods aimed at improving model outputs, such as DPOK [6] and DDPO [3]; and methods like DreamSync [26], which employ self-training strategy but focus on SFT stage. Given that these baseline methods are all conducted upon SD v1.4, we ensure a fair comparison by using the same version of the SD model as the foundation and employing the same VQA model (BLIP-2) for evaluation. Results reveal that our method AGFSync can simultaneously improve the text fidelity and visual quality of SD v1.4, SD v1.5, and SDXL models. For SD v1.4, AGFSync achieves an improvement of 1.3% of VQA score and 3.3% of aesthetic score, with a sum of 4.6% improvement on the TIFA benchmark, higher than all baseline models. Notice that although DPOK shows a 1.9% improvement on aesthetic score, it reduces the model’s text faithfulness through VQA score. For SD v1.5 and SDXL, our method AGFSync leads to improvements of 1.6% and 1.1% for SD v1.5, 1.3% and 4.3% for SDXL in terms of VQA score and aesthetic score respectively.

### 5.3 Ablation Experiment of Multi-Aspect Scoring

**Table 2:** Results of the ablation study of applied scoring measures. Experiments are conducted with SD v1.5 on TIFA.

Applied Measures				$s_{\text{CLIP}}$	$s_{\text{VQA}}$	$s_{\text{Aes.}}$
+CLIP	+VQA	+Aes.	+Pick			
-	-	-	-	27.0	77.1	48.0
✓	-	-	-	<b>27.2</b>	<b>77.7</b>	<b>47.3</b>
-	✓	-	-	<b>27.1</b>	<b>77.4</b>	<b>45.7</b>
-	-	✓	-	27.0	<b>76.8</b>	<b>48.6</b>
✓	✓	-	-	<b>27.2</b>	<b>77.5</b>	<b>47.0</b>
✓	-	✓	-	<b>27.2</b>	<b>77.8</b>	<b>47.2</b>
-	✓	✓	-	<b>27.1</b>	<b>77.2</b>	<b>48.2</b>
-	-	-	✓	<b>27.1</b>	<b>78.0</b>	<b>47.8</b>
✓	✓	✓	-	<b>27.3</b>	<b>78.7</b>	<b>49.1</b>

**Table 3:** The number of prompts of different categories and the total number of prompts in our dataset.

Category	Count
Natural Landscapes	5733
Cities and Architecture	6291
People	5035
Animals	3089
Plants	4276
Food and Beverages	3010
Sports and Fitness	2994
Art and Culture	2432
Technology and Industry	3224
Everyday Objects	2725
Transportation	4450
Abstract and Conceptual	2575
Total	45834

As depicted in Tab. 2, to validate the efficacy of the three scores we employed for image quality assessment, we conduct a thorough ablation study. We train the

SD v1.5 model on preference datasets constructed with different combinations of the three scores, along with PickScore [11]. As in AGFSync, with training model on preference datasets built using a combination of CLIP score, VQA score, and aesthetic score result in the greatest improvement across all three metrics. While other combinations often show a decrease in certain metric rather than a consistent improvement on all metrics.

#### 5.4 Qualitative Comparison of Faithfulness and Coherence

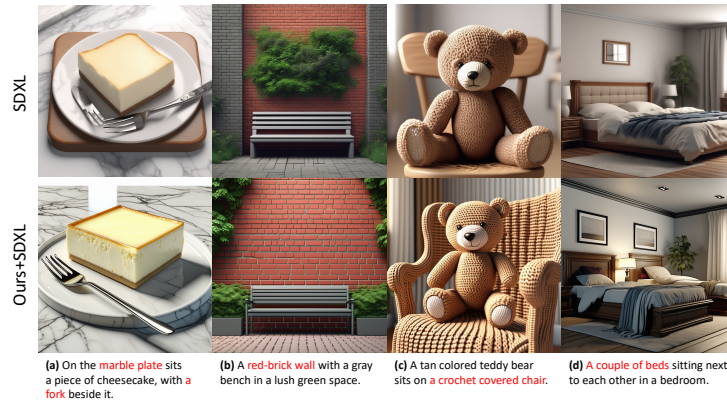


**Fig. 5:** Text faithfulness comparisons between SDXL and AGFSync (Ours)+SDXL. The top row shows images generated by SDXL, while the second row displays images generated by Ours+SDXL. In the descriptions at the bottom, the **red-highlighted** portions indicate discrepancies between images generated by SDXL and input prompts.

To visually demonstrate the improvement of AGFSync, we present comparisons of the SDXL model along with AGFSync for the same image description in Fig. 5 and Fig. 6. From Fig. 5, we observe that while the original SDXL model can generate vivid images, there are instances where discrepancies arise between the generated image and the input description. After fine-tuning with AGFSync, the SDXL model generates images that are more consistent with the input description. Additionally, in Fig. 6, we notice that the original SDXL model sometimes generates images that deviate from real-world patterns or physical logic in certain details, whereas the fine-tuned SDXL model with AGFSync performs better in such cases. For instance, in the second column, the girl’s chest generated by SDXL exhibits unrealistic wrinkles, while in the fourth column, the top cake appeared suspended during stacking.

#### 5.5 Prompt Utilization Rate Analysis

To compare with DreamSync [26], in Fig. 7, we present the number of prompts that can be selected from our generated dataset as the thresholds for VQA score

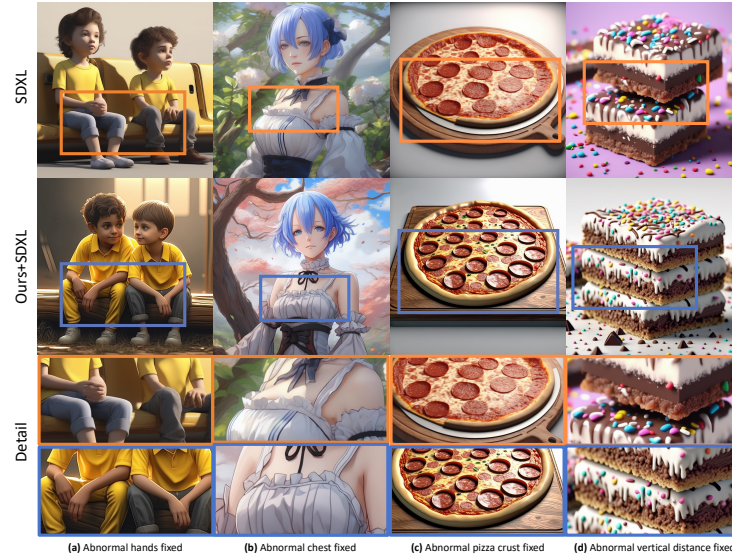


**Fig. 6:** Comparison of adherence to real-world rules between SDXL and AGFSync (Ours)+SDXL. The first row shows the images generated by SDXL, while the second row displays those generated by Ours+SDXL. The third row illustrates the comparison of details between the two, demonstrating AGFSync’s finer coherence and details.

and aesthetic Score vary. Specifically, these are prompts for which at least one generated image scores above the respective thresholds. With DreamSync’s 0.9 and 0.6 thresholds for two metrics, only 48.8% of prompts satisfying both, meaning a low data conversion efficiency of 48.8% on our dataset. However, AGFSync’s approach merely requires selecting the best and worst images without imposing any threshold constraints, thereby achieving a data conversion efficiency of 100%.

## 6 Limitations

Firstly, AGFSync relies on existing large language models (LLMs) and aesthetic scoring models, whose performance and accuracy could be influenced by the biases and limitations of the LLMs. Secondly, while we introduce random noise to increase image diversity, this method might lead to a reduction in consistency between some images and their text prompts. In addition, due to the high cost of time or money, we have not adopted LLaVA [13], GPT-4V and latest advanced multimodal large models [4, 13, 18, 29, 33, 34] to generate prompts or QA pairs. In terms of image evaluation, we employ VQA scores, CLIP scores, and aesthetic scores, which may not capture all aspects of image quality.

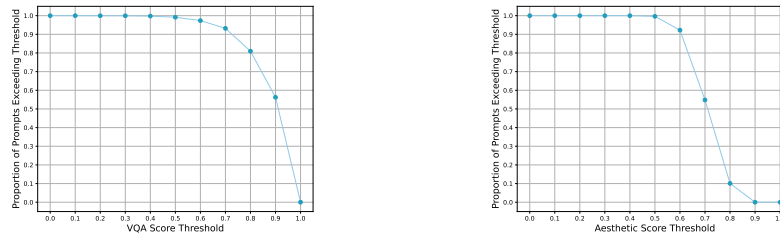


**Fig. 7:** In our generated dataset constructed with images generated by SDXL, the proportion of prompts that can be filtered out based on varying thresholds.

## 7 Conclusions

Our proposed text-to-image generation framework **AGFSync**, by leveraging Direct Preference Optimization (DPO) and multi-aspect AI feedback, significantly enhances the prompt following ability and image quality regarding style, coherence, and aesthetics. Extensive experiments on the HPSv2 and TIFA benchmark demonstrate that **AGFSync** outperforms baseline models in terms of VQA scores, CLIP score, aesthetic evaluation. Based on an AI-driven feedback loop, **AGFSync** eliminates the need for costly human-annotated data and manual intervention, paving the way for scalable alignment techniques.

## References

1. Achiam, J., Adler, S., Agarwal, S., Ahmad, L., Akkaya, I., Aleman, F.L., Almeida, D., Altenschmidt, J., Altman, S., Anadkat, S., et al.: Gpt-4 technical report. arXiv preprint arXiv:2303.08774 (2023)
2. Betker, J., Goh, G., Jing, L., Brooks, T., Wang, J., Li, L., Ouyang, L., Zhuang, J., Lee, J., Guo, Y., et al.: Improving image generation with better captions. Computer Science. <https://cdn.openai.com/papers/dall-e-3.pdf> **2**(3), 8 (2023)
3. Black, K., Janner, M., Du, Y., Kostrikov, I., Levine, S.: Training diffusion models with reinforcement learning. arXiv preprint arXiv:2305.13301 (2023)
4. Dai, W., Li, J., Li, D., Tiong, A.M.H., Zhao, J., Wang, W., Li, B., Fung, P., Hoi, S.: Instructblip: Towards general-purpose vision-language models with instruction tuning (2023)
5. Dai, X., Hou, J., Ma, C.Y., Tsai, S., Wang, J., Wang, R., Zhang, P., Vandenhende, S., Wang, X., Dubey, A., Yu, M., Kadian, A., Radenovic, F., Mahajan, D., Li, K., Zhao, Y., Petrovic, V., Singh, M.K., Motwani, S., Wen, Y., Song, Y., Sumbaly, R., Ramanathan, V., He, Z., Vajda, P., Parikh, D.: Emu: Enhancing image generation models using photogenic needles in a haystack (2023)
6. Fan, Y., Watkins, O., Du, Y., Liu, H., Ryu, M., Boutilier, C., Abbeel, P., Ghavamzadeh, M., Lee, K., Lee, K.: Reinforcement learning for fine-tuning text-to-image diffusion models. *Advances in Neural Information Processing Systems* **36** (2024)
7. Feng, W., He, X., Fu, T.J., Jampani, V., Akula, A., Narayana, P., Basu, S., Wang, X.E., Wang, W.Y.: Training-free structured diffusion guidance for compositional text-to-image synthesis (2023)

8. Hessel, J., Holtzman, A., Forbes, M., Bras, R.L., Choi, Y.: Clipscore: A reference-free evaluation metric for image captioning. arXiv preprint arXiv:2104.08718 (2021)
9. Hu, Y., Liu, B., Kasai, J., Wang, Y., Ostendorf, M., Krishna, R., Smith, N.A.: Tifa: Accurate and interpretable text-to-image faithfulness evaluation with question answering. arXiv preprint arXiv:2303.11897 (2023)
10. Ke, J., Ye, K., Yu, J., Wu, Y., Milanfar, P., Yang, F.: Vila: Learning image aesthetics from user comments with vision-language pretraining. In: Proceedings of the IEEE/CVF Conference on Computer Vision and Pattern Recognition. pp. 10041–10051 (2023)
11. Kirstain, Y., Polyak, A., Singer, U., Matiana, S., Penna, J., Levy, O.: Pick-a-pic: An open dataset of user preferences for text-to-image generation. Advances in Neural Information Processing Systems **36** (2024)
12. Li, J., Li, D., Savarese, S., Hoi, S.: Blip-2: bootstrapping language-image pre-training with frozen image encoders and large language models. In: Proceedings of the 40th International Conference on Machine Learning. ICML'23, JMLR.org (2023)
13. Liu, H., Li, C., Wu, Q., Lee, Y.J.: Visual instruction tuning (2023)
14. OpenAI: Introducing chatgpt (2023)
15. Ouyang, L., Wu, J., Jiang, X., Almeida, D., Wainwright, C., Mishkin, P., Zhang, C., Agarwal, S., Slama, K., Ray, A., et al.: Training language models to follow instructions with human feedback. Advances in Neural Information Processing Systems **35**, 27730–27744 (2022)
16. Pichai, S., Hassabis, D.: Introducing gemini: our largest and most capable ai model. Google. Retrieved December 8, 2023 (2023)
17. Podell, D., English, Z., Lacey, K., Blattmann, A., Dockhorn, T., Müller, J., Penna, J., Rombach, R.: Sdxl: Improving latent diffusion models for high-resolution image synthesis. arXiv preprint arXiv:2307.01952 (2023)
18. Qin, Y., Zhou, E., Liu, Q., Yin, Z., Sheng, L., Zhang, R., Qiao, Y., Shao, J.: Mp5: A multi-modal open-ended embodied system in minecraft via active perception. arXiv preprint arXiv:2312.07472 (2023)
19. Radford, A., Kim, J.W., Hallacy, C., Ramesh, A., Goh, G., Agarwal, S., Sastry, G., Askell, A., Mishkin, P., Clark, J., et al.: Learning transferable visual models from natural language supervision. In: International conference on machine learning. pp. 8748–8763. PMLR (2021)
20. Rafailov, R., Sharma, A., Mitchell, E., Ermon, S., Manning, C.D., Finn, C.: Direct preference optimization: Your language model is secretly a reward model (2023)
21. Rassin, R., Hirsch, E., Glickman, D., Ravfogel, S., Goldberg, Y., Chechik, G.: Linguistic binding in diffusion models: Enhancing attribute correspondence through attention map alignment. Advances in Neural Information Processing Systems **36** (2023)
22. Rombach, R., Blattmann, A., Lorenz, D., Esser, P., Ommer, B.: High-resolution image synthesis with latent diffusion models. In: Proceedings of the IEEE/CVF conference on computer vision and pattern recognition. pp. 10684–10695 (2022)
23. Rombach, R., Blattmann, A., Lorenz, D., Esser, P., Ommer, B.: High-resolution image synthesis with latent diffusion models (2022)
24. Schuhmann, C.: Laion-aesthetics. <https://laion.ai/blog/laion-aesthetics/> (2022), accessed: 2024-02-29
25. Segalis, E., Valevski, D., Lumen, D., Matias, Y., Leviathan, Y.: A picture is worth a thousand words: Principled recaptioning improves image generation. arXiv preprint arXiv:2310.16656 (2023)

26. Sun, J., Fu, D., Hu, Y., Wang, S., Rassin, R., Juan, D.C., Alon, D., Herrmann, C., van Steenkiste, S., Krishna, R., Rashtchian, C.: Dreamsyntax: Aligning text-to-image generation with image understanding feedback (2023)
27. Wallace, B., Dang, M., Rafailov, R., Zhou, L., Lou, A., Purushwalkam, S., Ermon, S., Xiong, C., Joty, S., Naik, N.: Diffusion model alignment using direct preference optimization (2023)
28. Wu, X., Hao, Y., Sun, K., Chen, Y., Zhu, F., Zhao, R., Li, H.: Human preference score v2: A solid benchmark for evaluating human preferences of text-to-image synthesis. arXiv preprint arXiv:2306.09341 (2023)
29. Ye, Q., Xu, H., Xu, G., Ye, J., Yan, M., Zhou, Y., Wang, J., Hu, A., Shi, P., Shi, Y., et al.: mplug-owl: Modularization empowers large language models with multimodality. arXiv preprint arXiv:2304.14178 (2023)
30. Zhang, C., Zhang, C., Zhang, M., Kweon, I.S.: Text-to-image diffusion model in generative ai: A survey. arXiv preprint arXiv:2303.07909 (2023)
31. Zhang, L., Rao, A., Agrawala, M.: Adding conditional control to text-to-image diffusion models. In: Proceedings of the IEEE/CVF International Conference on Computer Vision. pp. 3836–3847 (2023)
32. Zhou, C., Liu, P., Xu, P., Iyer, S., Sun, J., Mao, Y., Ma, X., Efrat, A., Yu, P., Yu, L., et al.: Lima: Less is more for alignment. Advances in Neural Information Processing Systems **36** (2024)
33. Zhou, E., Qin, Y., Yin, Z., Huang, Y., Zhang, R., Sheng, L., Qiao, Y., Shao, J.: Minedreamer: Learning to follow instructions via chain-of-imagination for simulated-world control. arXiv preprint arXiv:2403.12037 (2024)
34. Zhu, D., Chen, J., Shen, X., Li, X., Elhoseiny, M.: Minigt-4: Enhancing vision-language understanding with advanced large language models. arXiv preprint arXiv:2304.10592 (2023)

## Appendix

### A Notations

The notations and their descriptions in the paper are shown in Tab. 4.

### B Experimental Environments and Settings

The parameters and devices used for sampling and training are displayed in Tab. 5.

### C Efficiency of AGFSync Illustration

Tab. 6 presents a comprehensive overview of the time required to apply our methodology AGFSync across various stages and models, specifically delineating the durations for tasks such as prompt and QA generation, image generation, VQA scoring, combined CLIP and Aesthetic scoring, and model training. We compare these processes across SD v1.4, SD v1.5, and SDXL models. For prompt

**Table 4:** Notations symbols and their descriptions

Notations	Descriptions
$\mathbf{c}, \mathbf{c}^{(emb)}$	LLM-generated text prompt and its embedding
$G$	T2I diffusion model
$\mathbf{n}$	Gaussian noise
$\mathbf{z}_0$	latent space noise in diffusion model
$\mathbf{x}_t^i$	the $i$ -th diffusion model generated image of step $t$
$(Q_i(\mathbf{c}), A_i(\mathbf{c}))$	$i$ -th question-answer pair for text prompt $\mathbf{c}$
$N_{\mathbf{c}}$	the number of question-answer pairs
$\gamma$	weight term in CLIP score
$s_{\square}$	score to evaluate image quality, footnote $\square$ is the name of the score
$W = \{w_1, w_2, \dots\}$	weights set for each score measurements
$S$	weighted score that evaluate multi-aspect image quality
$\Phi$	VQA Model

**Table 5:** More experimental details of AGFSync.

Number of Inference Steps	50
Images per Prompt	8
Sampling Precision	FP16
SDXL Resolution	$1024 \times 1024$
SD v1.4 & SD v1.5 Resolution	$512 \times 512$
SDXL Batch Size	64
SD v1.4 & SD v1.5 Batch Size	128
Max Training Steps	1000
SDXL Learning Rate	0.000001
SD v1.4 & SD v1.5 Learning Rate	0.0000005
Learning Rate Scheduler	Cosine
Mixed Precision	FP16
GPUs for Training	$8 \times \text{NVIDIA A100}(80\text{G})$

**Table 6:** Approximate time consumption of AGFSync across various stages and models.

Model	Prompt & QA Gen.	Image Gen.	VQA Score	CLIP Score & Aes. Score	Training
SD v1.4	12h	6h	7h	44 min	1.5h
SD v1.5					
SDXL		13h	12h		

and QA generation, all three models require a uniform duration of 12 hours. Image generation and VQA scoring demonstrate variability, with SD v1.4 and SD v1.5 completing in 6 and 7 hours respectively, which contrasts with SDXL’s longer durations of 13 and 12 hours for these tasks. The evaluation of CLIP and



Aesthetic scores takes a relatively shorter time, consistently taking 44 minutes across all models. Training times show a distinction between the models, with SD v1.4 and SD v1.5 requiring only 1.5 hours, whereas SDXL necessitates a longer commitment of 3 hours. Tab. 6 underscores the efficiency and resource requirements of our method when applied to different models, providing insightful benchmarks for planning and resource allocation.

## D Complementary Experiments

### D.1 SDXL Refiner Performance in TIFA Benchmark

We also applied our method to the SDXL+Refiner model, conducting 40 inference steps on the SDXL model followed by 10 inference steps using the Refiner model. Utilizing the same random seed, the results on the TIFA benchmark are shown in Tab. 7.

**Table 7:** Results of SDXL+Refiner and AGFSync (Ours)+SDXL+Refiner for VQA score and Aesthetic score on the TIFA benchmark. **Red** indicates improvement, while **Green** indicates a decrease. The best scores for each model type are highlighted in **Bold**. Column "Sum" denotes the sum of improvements on  $s_{VQA}$  and  $s_{Aes}$ .

Model	Alignment	$s_{VQA}$	$s_{Aes}$	Sum
SDXL + Refiner	No alignment	82.8	61.4	-
	AGFSync (Ours)	<b>83.9 (+1.1)</b>	<b>64.1(+3.7)</b>	<b>+4.8</b>

### D.2 Analysis of Prompts Filtering for High-Quality Image Generation

We also employed the method described in "DreamSync" to filter prompts capable of generating high-quality images from our generated prompts. Specifically, we filtered prompts that could generate images with a VQA score  $> 0.9$  and an Aesthetic score  $> 0.6$  using the SD v1.5 model. Tab. 8 presents the attributes of the text and the questions generated from the filtered prompts, while Tab. 9 displays the number and proportion of each category of prompts obtained through filtering. The results indicate that, although there is no significant change in the nature of the text and the generated questions of the filtered prompts, the proportion of filtered prompts varies greatly across different categories, with the difference in filtering proportion reaching up to 33.5%. This suggests that the types of prompts that the SD v1.5 model, or T2I models in general, excel at vary significantly across categories. Merely selecting prompts capable of producing high-quality images for training is insufficient for a comprehensive approach.

**Table 8:** In our dataset, statistics of prompts that can generate images with VQA score  $> 0.9$  and Aesthetic score  $> 0.6$  through the SD v1.5 model.

Statistic	Value
Total number of prompts	15,262
Total number of questions	132,893
Average number of questions per prompt	8.71
Average number of words per prompt	26.75
Average number of elements in prompts	8.05
Average number of words per question	7.94

**Table 9:** In our dataset, the number of various categories of prompts that can generate images with VQA Score  $> 0.9$  and Aesthetic Score  $> 0.6$  through the SD v1.5 model, and their retention proportions compared to the original categories of prompts.

Category	Count	Retention Proportion
Natural Landscapes	1992	34.7%
Cities and Architecture	2046	32.5%
People	1950	38.7%
Animals	1347	43.6%
Plants	1849	43.2%
Food and Beverages	1116	37.1%
Sports and Fitness	1060	35.4%
Art and Culture	714	29.4%
Technology and Industry	853	26.5%
Everyday Objects	712	26.1%
Transportation	1362	30.6%
Abstract and Conceptual	261	10.1%

### D.3 Results of Training Models with Different Amounts of Data

Our preference dataset construction method achieved a 100% data conversion efficiency, highlighting the importance of high data conversion efficiency. To further demonstrate this, we randomly selected different proportions of data from our dataset for experiments. Moreover, following the strategy introduced in "Dream-Sync", we filtered prompts capable of generating high-quality images based on two sets of thresholds (VQA score  $> 0.85$  and Aesthetic score  $> 0.5$ , and VQA score  $> 0.9$  and Aesthetic score  $> 0.6$ ) to construct a preference dataset for training, using SD v1.5 as the base model and conducting the experiment on the TIFA benchmark. The experimental results are shown in Tab. 10. The results indicate that although the Aesthetic scores surpassed the scenario of using all data when trained with 60% and 80% of the data, considering the CLIP score, VQA score, and Aesthetic score together, the larger the volume of data, the better the overall performance of the model. Especially, the improvement in model performance when increasing data usage from 60% to 100% is significantly greater

than that from 0% to 60%. Notably, with only our limited constructed preference dataset (i.e. 20% of the preference dataset), we had significant improvements in all aspects, further demonstrating AGFSync’s efficiency.

**Table 10:** Evaluation results of training the SD v1.5 model with different amounts of data on the TIFA benchmark. The second column shows the method used for data selection. Red indicates improvement relative to the original SD v1.5, while green indicates a decrease. We highlight the highest score in each column in bold.

Proportion	Sample Method	$s_{CLIP}$	$s_{VQA}$	$s_{Aes.}$
0	-	27.0	77.1	48.0
20%	Random Sample	27.2(+0.2)	77.4(+0.3)	49.1(+1.1)
33.3%	$s_{VQA} > 0.9, s_{Aes.} > 0.6$	27.1(+0.1)	77.4(+0.3)	49.1(+1.1)
40%	Random Sample	27.1(+0.1)	77.5(+0.4)	48.8(+0.8)
60%	Random Sample	27.1(+0.1)	77.6(+0.5)	<b>49.3(+1.3)</b>
60.6%	$s_{VQA} > 0.85, s_{Aes.} > 0.5$	<b>27.3(+0.3)</b>	77.7(+0.6)	47.6(-0.4)
80%	Random Sample	<b>27.3(+0.3)</b>	78.3(+1.2)	49.2(+1.2)
100%	-	<b>27.3(+0.3)</b>	<b>78.7(+1.6)</b>	49.1(+1.1)

## E LLM and VLM Instructions Details

### E.1 Example Instruction to Generate Image Caption

Using LLM to generate image captions is the first step in constructing a dataset. In this step, we use GPT-3.5 to generate diverse image captions. When generating captions, we specify the category of the caption and provide five examples. Below is an example of an instruction:

*You are a large language model, trained on a massive dataset of text. You can generate texts from given examples. You are asked to generate similar examples to the provided ones and follow these rules:*

1. *Your generation will be served as prompts for Text-to-Image models. So your prompt should be as visual as possible.*
2. *Do NOT generate scary prompts.*
3. *Do NOT repeat any existing examples.*
4. *Your generated examples should be as creative as possible.*
5. *Your generated examples should not have repetition.*
6. *Your generated examples should be as diverse as possible.*
7. *Do NOT include extra texts such as greetings.*
8. *Generate {num} descriptions.*

9. *The descriptions you generate should have a diverse word count, with both long and short lengths.*
10. *The more detailed the description of an image, the better, and the more elements, the better.*

*Please open your mind based on the theme "Natural Landscapes: Includes terrain, bodies of water, weather phenomena, and natural scenes." paintings  
Here are five example descriptions for natural landscape images:*

1. *A sprawling meadow under a twilight sky, where the last rays of the sun kiss the tips of wildflowers, creating a canvas of gold and purple hues.*
2. *A majestic waterfall cascading down rugged cliffs, enveloped by a mist that dances in the air, surrounded by an ancient forest whispering the tales of nature.*
3. *An endless desert, where golden dunes rise and fall like waves in an ocean of sand, punctuated by the occasional resilient cactus standing as a testament to life's perseverance.*
4. *A serene lake, mirror-like, reflecting the perfect image of surrounding snow-capped mountains, while a solitary swan glides gracefully, leaving ripples in its wake.*
5. *The aurora borealis illuminating the polar sky in a symphony of greens and purples, arching over a silent, frozen landscape that sleeps under a blanket of snow.*

*Please imitate the example above to generate a diverse image description and do not repeat the example above.*

*Each description aims to vividly convey the beauty and unique atmosphere of various natural landscapes.*

*The format of your answer should be:*

```
{  
  "descriptions": [...]  
}
```

*Ensure that the response can be parsed by `json.loads` in Python, for example: no trailing commas, no single quotes, and so on.*

## **E.2 Instruction to Generate Question and Answer Pairs with Validation**

After obtaining a large number of image captions, we also need to break these captions down into Question-Answer (QA) pairs. For this step, we use Gemini Pro, requesting it to decompose each image caption into 15 QA pairs, with each caption processed six times. Finally, we filter out the QA pairs that were generated repeatedly. Below is the instruction given to Gemini Pro for breaking down image captions into QA pairs.

*You are a large language model, trained on a massive dataset of text. You can receive the text as a prompt for Text-to-Image models and break it down into*

general interrogative sentences that verifies if the image description is correct and give answers to those questions.

You must follow these rules:

1. Based on the text content, the answers to the questions you generate must only be 'yes', meaning the questions you generate should be general interrogative sentences.
2. The questions you generate must have a definitive and correct answer that can be found in the given text, and this answer must be 'yes'.
3. The correct answer to your generated question cannot be unmentioned in the text, nor can it be inferred solely from common sense; it must be explicitly stated in the text.
4. Each question you break down from the text must be unique, meaning that each question must be different.
5. If you break down the text into questions, each question must be atomic, i.e., they must not be divided into new sub-questions.
6. Categorize each question into types (object, human, animal, food, activity, attribute, counting, color, material, spatial, location, shape, other).
7. You must generate at least 15 questions, ensuring there are at least 15 question ids.
8. The questions you generate must cover the content contained in the text as much as possible.
9. You also need to indicate whether the question you provided is an invalid question of the "not mentioned in the text" type, with 0 representing an invalid question and 1 representing a minor question.

Each time I'll give you a text that will serve as a prompt for Text-to-Image models.

You should only respond in JSON format as described below:

```
[
  {
    "question_id": "The number of the issue you generated
    ↪ , starting with 1",
    "question": "A general interrogative sentence you
    ↪ derive from breaking down the text should
    ↪ inquire whether the image conforms to the
    ↪ content of the text. The answer to this
    ↪ question must be found based on the text, not
    ↪ on common sense, etc. The answer must not be
    ↪ unmentioned in the text, and according to the
    ↪ text, the answer to this question must be 'yes
    ↪ '.",
    "answer": "The real answer to the question according
    ↪ to the text provided. The answer should be '
    ↪ yes'",
    "element_type": "The type of problem. (object, human,
    ↪ animal, food, activity, attribute, counting,
    ↪ color, material, spatial, location, shape,
    ↪ other)",
```

```

    "element": "The elements mentioned in the question,
    ↪ or the specific elements asked by the question
    ↪ ",
    "flag": "Check if the correct answer to the question
    ↪ you generated is an invalid question such as
    ↪ not mentioned, with 0 being an invalid
    ↪ question and 1 being not an invalid question"
  }
  # There should be more questions here, because a text
  ↪ should be broken down into multiple questions, and
  ↪ the number of questions is up to you
]

```

Ensure that the response can be parsed by `json.loads` in Python, for example: no trailing commas, no single quotes, and so on.

### E.3 Detailed Instruction When Using GPT-4V for Evaluation

When evaluating the model trained with our method using GPT-4V, to allow GPT-4V to decide whether the image generated by the post-training model is better or the one generated by the original model is better, we designed the following instruction:

*The prompt for these two pictures is: {prompt} Which image do you prefer? No matter what happens, you must make a choice and answer A or B.*

*Reply in JSON format below:*

```

{
  "reason": "your reason",
  "choice": "A/B"
}

```

*Which image better fits the text description? No matter what happens, you must make a choice and answer A or B.*

*Reply in JSON format below:*

```

{
  "reason": "your reason",
  "choice": "A/B"
}

```

*Disregarding the prompt, which image is more visually appealing? No matter what happens, you must make a choice and answer A or B.*

*Reply in JSON format below:*

```

{
  "reason": "your reason",
  "choice": "A/B"
}

```

## F Details of Generated Prompts and Preference Dataset

### F.1 Statistics of the AI-Generated Captions

Tab. 11 presents more detailed data of our generated dataset. In addition to this, in our generated QA pairs, the counts for each category are as follows: shape (2385), counting (3809), material (4495), food (4660), animal (5533), color (12749), human (17921), spatial (21878), other (24513), location (42914), object (77783), activity (83712), and attribute (101713).

**Table 11:** Summary Statistics of QA Pair Dataset

Statistic	Value
Total number of prompts	45,834
Total number of questions	414,172
Average number of questions per prompt	9.03
Average number of words per prompt	26.061
Average number of elements in prompts	8.22
Average number of words per question	8.07

### F.2 Example Generated Image Caption and Corresponding QA Pairs

For the example prompt: *A vast, open savannah, where golden grasses sway in the wind, dotted with acacia trees and herds of majestic elephants and giraffes, as the sun sets on the horizon.* We have the corresponding QA pairs as in Tab. 12. As indicated in Tab. 12, for each generated question, we require the LLM to provide the main element and type of element being asked in the question.

### F.3 Example Preference Dataset Generated by AGFSync

As shown in Fig. 8, each data set consists of a high-quality image, a lower-quality image, and a corresponding image caption.



**Table 12:** Example of corresponding QA pairs.

<b>Question and Choices</b>	<b>Type</b>	<b>Element</b>
Q: Is there a vast, open savanna in the image? A: Yes	location	savannah
Q: Is there golden grass in the savannah? A: Yes	object	golden grass
Q: Do golden grasses sway in the wind in the described scene? A: Yes	activity	golden grasses
Q: Is there a mention of acacia trees in the image? A: Yes	object	acacia trees
Q: Are there majestic elephants in the savannah? A: Yes	animal	elephants
Q: Are the giraffes majestic? A: Yes	attribute	giraffes
Q: Is there a sun setting on the horizon? A: Yes	activity	sun setting

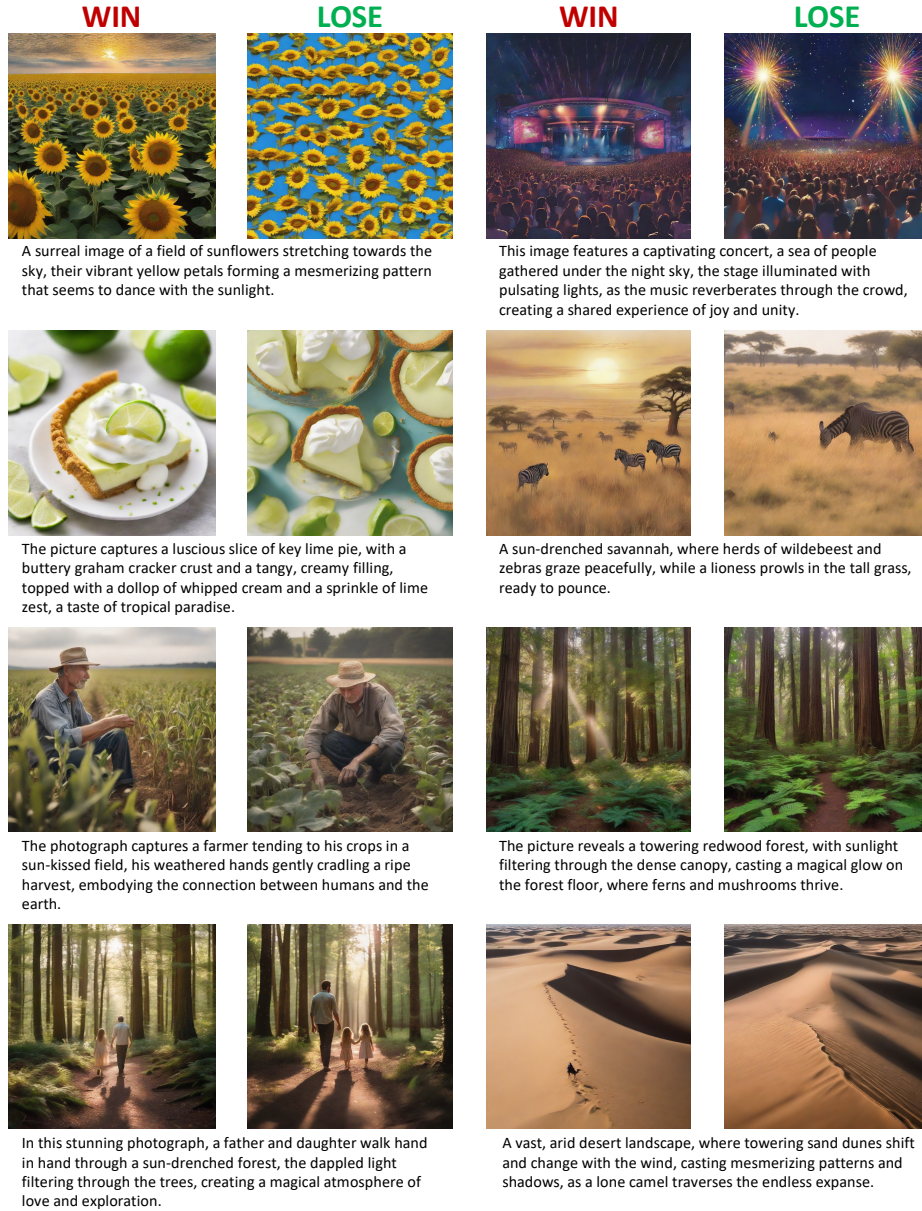


**Fig. 8:** Some examples of the preference dataset we generated.